Solitons in fibers with loss beyond small perturbation

Fedor Mitschke,* Alexander Hause, and Christoph Mahnke
Universität Rostock, Institut für Physik, Albert-Einstein-Straße 23, 18059 Rostock, Germany
(Received 16 March 2017; published 13 July 2017)

We consider the evolution of fiber-optic solitons in the presence of loss. Localized power reduction can be cast into a well-known form for which changes of all parameters are known explicitly. We proceed to a sequence of such perturbations with the same total loss, so that still all parameters are known, and eventually take the limit to infinitely many steps. This establishes the connection with distributed loss, and in the limit of vanishing loss reproduces the known results from perturbation theory. Outside this adiabatic limit the mechanism becomes clear that causes deviations: interference between solitons and radiation upsets the balance of dispersive and nonlinear effects characteristic of solitons; as one consequence the soliton continually sheds energy, which goes into radiation. We derive an expression for the radiation production rate in a lossy fiber, and predict quantitatively the distance until the soliton finally decays. Our approach provides quantitative results for fibers with loss small or strong, localized or distributed, and numerical results confirm predictions. It can be generalized to gain rather than loss.

DOI: 10.1103/PhysRevA.96.013826

I. INTRODUCTION

The nonlinear Schrödinger equation (NLSE) is a nonlinear wave equation with numerous fields of application, including certain water surface waves, plasma waves, and the dynamics of Bose-Einstein condensates. It is also central to all modeling of nonlinear light pulse propagation in optical fiber. Numerous correction terms have been added for the latter case, to make the model more precise, or more widely applicable.

The fact that the NLSE (without additional terms) is integrable allowed Zakharov and Shabat to find its soliton solution [1] by the inverse scattering technique: a wave of just the right shape can propagate stably in spite of, or indeed due to, the nonlinearity. Satsuma and Yajima [2] treated the initial value problem associated with the soliton solution: How do initial shape perturbations evolve? Hasegawa and Tappert pointed out that light pulse propagation in optical fiber, a novelty at the time, would obey the NLSE, and that there would be stable soliton pulses [3]. A first experimental demonstration was given [4], and approximately 20 years later the concept was introduced to commercial fiber-optic transmission systems with live data [5].

A real-world system is not described very accurately by the NLSE in its original form. The first correction to it is a loss term because there is no such thing as a perfectly lossless fiber. Even when optical amplifiers are added, loss is canceled on path average, but not at every point. A loss term, however, destroys the integrability, and it is not immediately clear what happens to the soliton concept. There have been several studies of this question, typically with perturbation approaches [6–11]. However, the assumption that the loss is small is a severe restriction, and for realistic losses the obtained prediction is inaccurate [12].

Our approach to a near soliton in a lossy environment does not suffer from that restriction. It is applicable also to strong loss, all the way to the decay of the soliton into radiation, and it can also be applied to the case of gain. The core idea is that we consider the loss along the fiber as the limit of a sequence of very small stepwise losses in an otherwise lossless fiber. In this way we can cast the problem such that the Satsuma-Yajima initial value problem can be used to predict analytically what happens at each step. We then have to take care of the radiation generated at each step, and the way the individual contributions add up or interfere. To this end we present a description of the soliton-radiation beat, which is much more complete than the original statement of Satsuma and Yajima [2] and later contributions [13,14], even though we still make one approximation.

For brevity and clarity we restrict ourselves to the case of a single soliton. We first recast the findings of Refs. [1] and [2] into a more transparent, modern form, which follows much of the now established terminology (as used, e.g., in Refs. [15,16]). However, we write equations not in dimensionless form but with physical parameters. While the former is undoubtedly more elegant mathematically, the latter is more useful to connect to physical insight.

II. KNOWN FACTS

In the nonlinear Schrödinger equation with physical quantities [15,16]

$$i\frac{\partial}{\partial z}A - \frac{\beta_2}{2}\frac{\partial^2}{\partial t^2}A + \gamma|A|^2A = 0, \tag{1}$$

$A(z,t)$ is the pulse envelope referred to a frame of reference moving with the group velocity that pertains to the optical carrier frequency. β_2 is the coefficient of group velocity dispersion, and γ the coefficient of nonlinearity. If centered in a comoving frame of reference, the solution now known as the fundamental soliton takes the form

$$A(z,t) = \sqrt{\frac{|\beta_2|}{\gamma}}\,\frac{1}{T_0}\,\mathrm{sech}\!\left(\frac{t}{T_0}\right)\exp\!\left(i\frac{|\beta_2|z}{2T_0^2}\right), \tag{2}$$

where T_0 is the pulse duration. The prefactor of the sech term in Eq. (2) sets the peak amplitude and can be written as

$$A_{\max} = \sqrt{\frac{|\beta_2|}{\gamma}}\,\frac{1}{T_0} = \sqrt{P_0}. \tag{3}$$

By convenient convention amplitudes are scaled so they can be written as square root of power. It follows that the solution

*fedor.mitschke@uni-rostock.de

is constrained by

$$P_0 T_0^2 = \frac{|\beta_2|}{\gamma}. \tag{4}$$

Integration yields the soliton energy as

$$E_{\rm sol} = 2 P_0 T_0. \tag{5}$$

This energy is preserved because no loss is considered in Eq. (1).

For later use we quote the characteristic length scales of dispersion and nonlinearity commonly defined as

$$L_{\rm D} = \frac{T_0^2}{|\beta_2|} \quad \text{and} \quad L_{\rm NL} = \frac{1}{\gamma P_0}. \tag{6}$$

For a soliton, $L_{\rm D} = L_{\rm NL}$. From Eq. (2) it is immediately obvious that the phase term rotates through 2π over a distance

$$z_{2\pi} = 4\pi L_{\rm D} = 4\pi L_{\rm NL}. \tag{7}$$

To quantify a deviation from the exact soliton solution we can use the soliton order $N \geqslant 0$, $N \in \mathbb{R}$. N can be inserted as a multiplier on the right-hand side of Eq. (2); then, Eq. (4) is modified into

$$P_0 T_0^2 = N^2 \frac{|\beta_2|}{\gamma}. \tag{8}$$

A pulse with noninteger N cannot be a pure soliton. Rather, in such case there is a soliton plus a nonsolitonic remainder [1,2], which propagates as a linear (purely dispersive) wave known as radiation. If an unchirped sech-shaped pulse of the type

$$A(0,t) = N\sqrt{P_0}\,\mathrm{sech}\left(\frac{t}{T_0}\right) \tag{9}$$

is launched, it has energy

$$E_{\rm tot} = 2N^2 P_0 T_0 = N^2 E_{\rm sol}. \tag{10}$$

It follows from Ref. [2] that part of this goes into radiation, the remainder into a new soliton:

$$E_{\rm rad} = (N-1)^2\, E_{\rm sol} \quad \text{and} \quad E_1 = (2N-1)\, E_{\rm sol}. \tag{11}$$

The new soliton has $E_1 \neq E_{\rm sol}$, $P_1 \neq P_0$, and $T_1 \neq T_0$. Across the interval $1/2 \leqslant N \leqslant 3/2$, E_1 varies linearly from 0 to $2E_{\rm sol}$. For $N < 1/2$ no soliton exists; for $N > 3/2$ a second one appears. Here we restrict ourselves to $N < 3/2$. P_1 and T_1 follow from simultaneous solution of

$$P_1 T_1^2 = \frac{|\beta_2|}{\gamma} = P_0 T_0^2 \tag{12}$$

$$\text{and } P_1 T_1 = \frac{E_{\rm tot} - E_{\rm rad}}{2} = (2N-1) P_0 T_0 \tag{13}$$

$$\Rightarrow T_1 = \frac{T_0}{2N-1} \quad \text{and} \quad P_1 = (2N-1)^2\, P_0. \tag{14}$$

By virtue of integrability of the NLSE, no energy exchange occurs between solitons and radiation during copropagation. While both parts copropagate, their phase evolutions are different. The beating causes oscillations of both peak power and duration; they gradually subside after long propagation as the linear wave is dispersed away. Gordon [17] described this with a perturbational approach and spoke of the emergent soliton but emphasized that it exists from the beginning. Reference [18] presents a variational ansatz to describe the combination of soliton and radiation, and the damped beat note.

We obviously need to distinguish between the pulse and the soliton: soliton and radiation together form the pulse. From temporal and spectral pulse shapes alone one cannot tell the contributions apart. Direct scattering transform or DST provides a way to obtain that information; Osborne and Boffeta were the first to introduce a numerical version thereof [19]. That technique works on a numerically given temporal profile, and finds the eigenvalues characterizing soliton energies and velocities. We carefully assessed its numerical accuracy; by informed choice of discretization one can keep both truncation and sampling errors low. Moreover, as discussed in Ref. [20], a fourth-order Runge-Kutta integration scheme gives further improvement. In data shown below we obtain the energy to an accuracy of at least 10^{-8} and often better.

An alternative technique to find soliton parameters is soliton-radiation beat analysis. It works with arbitrary pulse shapes even when the system is nonintegrable [13,21]. That necessitates that the pulse shape used as an input to the algorithm must be provided not just at one particular position but over a certain representative segment of distance. By evaluating the evolution of the beat note between soliton and radiation both solitonic parameters and their change during propagation can be assessed. This way the eventual breakdown of a soliton in the presence of distributed loss was studied in Ref. [22]. In the Appendix we provide a much more detailed description of the beat.

III. INTRODUCING LOSS

Numerous articles were devoted to solitons in the presence of loss, mostly using perturbative approaches [6–11]. More recently, a Hirota approach has been presented [23], but unfortunately that work remains silent about the distinction between soliton and radiation.

Formally, one can insert a term $+(i/2)\,\alpha A$ on the left-hand side of Eq. (1), with α Beer's loss coefficient. According to Beer's law, the energy of a traveling pulse changes as $E(z) = E(0)\, e^{-\alpha Z}$. This describes distributed loss, which acts everywhere in the fiber. It is useful to introduce another characteristic length scale [compare Eq. (6)], the attenuation length

$$L_\alpha = \frac{1}{\alpha}. \tag{15}$$

Perturbation analysis predicts that when a soliton propagates through a fiber length Z and suffers an energy loss $e^{-\alpha Z}$ with $|\alpha Z| \ll 1$, the pulse width grows and its peak power wanes according to

$$T_{\rm sol} = T_0\, e^{+\alpha Z} \quad \text{and} \quad P_{\rm sol} = P_0\, e^{-2\alpha Z}. \tag{16}$$

This scaling was also confirmed numerically [25], but when the loss gets stronger, the errors become large [12].

Localized loss can arise in fiber joints such as connectors or splices, or even at sharp bends, etc.—we will speak of splices for short. Consider a pure soliton traveling down a loss-free fiber, hitting a splice, and thereafter moving on in a lossless fiber again. As the interaction distance involved in a

localized perturbation is zero, the attenuation can be described by multiplication of the pulse shape with a real constant, which we call Γ; for loss, $\Gamma < 1$. This assumes that the splice is gray (same attenuation across the spectral width of the pulse). Then we have a situation that is analytically tractable because, in a manner of speaking, it is piecewise integrable: it can be understood as a Satsuma-Yajima initial-value problem [2]. The parameters of the resulting pulse are found by interpretation of the attenuated pulse as an initial condition for the subsequent fiber. We denote the new parameters with indices Γ. E_Γ takes the place of the total energy $E_{\rm tot}$ from Eq. (10). The resulting pulse contains a soliton and some radiation. Its total energy is $E_\Gamma = \Gamma E_{\rm sol}$, and its shape is characterized by

$$P_\Gamma = \Gamma P_0 \quad \text{and} \quad T_\Gamma = T_0. \tag{17}$$

From

$$P_\Gamma T_\Gamma^2 = \Gamma P_0 T_0^2 = N^2 \frac{|\beta_2|}{\gamma} \tag{18}$$

we see that the resulting pulse is an N soliton with $N^2 = \Gamma$. This N is the value right after the splice; subsequently we decompose into soliton and radiation, and the new soliton has $N = 1$ in its own units.

We use Eqs. (10)–(11) and find that of the total remaining energy

$$E_{\rm tot}^{(\Gamma)} = N^2 E_{\rm sol} = \Gamma E_{\rm sol}, \tag{19}$$

[in order to avoid somewhat awkward double lower indices as in $E_{{\rm tot},\Gamma}$ we prefer upper indices (Γ)] the fraction going to radiation is

$$E_{\rm rad}^{(\Gamma)} = (\sqrt{\Gamma} - 1)^2 E_{\rm sol}. \tag{20}$$

The remaining energy

$$E_{\rm sol}^{(\Gamma)} = E_{\rm tot}^{(\Gamma)} - E_{\rm rad}^{(\Gamma)} = (2\sqrt{\Gamma} - 1) E_{\rm sol} \tag{21}$$

forms the new soliton, with both duration and peak power modified from Eq. (14):

$$T_{\rm sol}^{(\Gamma)} = \frac{T_\Gamma}{2\sqrt{\Gamma} - 1} = \frac{T_0}{2\sqrt{\Gamma} - 1}, x \tag{22a}$$

$$P_{\rm sol}^{(\Gamma)} = (2\sqrt{\Gamma} - 1)^2 P_\Gamma = (2\sqrt{\Gamma} - 1)^2 \Gamma P_0. \tag{22b}$$

It follows that after stepwise energy attenuation of the initial soliton with parameters P_0, T_0 by a factor $\Gamma \neq 1$ we get a soliton with parameters as in Eqs. (21), (22), along with some radiation energy as in Eq. (20). It is worthwhile to emphasize that the results for peak power and duration are different from the perturbative prediction, which refers to distributed loss: the latter can be written by identifying $\Gamma = e^{-\alpha Z}$ with fiber length Z and using Eq. (16) as $T_{\rm sol} = T_0/\Gamma$ and $P_{\rm sol} = \Gamma^2 P_0$. Obviously, it does make a difference whether the loss is distributed or localized.

We now let the loss described in the previous paragraph occur in two steps, i.e., at two splices. To keep the total attenuation constant, we assign each splice a loss factor of $\sqrt{\Gamma}$. Let us pretend for the moment that the two contributions to radiative energy can just be added to obtain the total radiation energy after the second splice. We will return to this assumption below, and subject it to scrutiny with some noteworthy insights.

In the discussion of the previous section we substitute $\Gamma \to \sqrt{\Gamma}$ and apply twice. We find a soliton energy of $E_{\rm sol}^{(\Gamma)}/E_{\rm sol} = (2\sqrt[4]{\Gamma} - 1)^2$, etc. Then we move on to consider loss occurring in a finite number n of steps. We substitute $(\Gamma \to \sqrt[n]{\Gamma})$ for each of n steps and obtain

$$\text{Soliton energy} \quad E_{\rm sol}^{(\Gamma)} = (2\sqrt[2n]{\Gamma} - 1)^n E_{\rm sol} \tag{23}$$

$$\text{Radiation energy} \quad E_{\rm rad}^{(\Gamma)} = (\sqrt[2n]{\Gamma} - 1)^{2n} E_{\rm sol} \tag{24}$$

$$\text{Soliton duration} \quad T_{\rm sol}^{(\Gamma)} = \frac{1}{(2\sqrt[2n]{\Gamma} - 1)^n} T_0 \tag{25}$$

$$\text{Soliton peak power} \quad P_{\rm sol}^{(\Gamma)} = (2\sqrt[2n]{\Gamma} - 1)^{2n} \Gamma P_0. \tag{26}$$

Finally we let $n \to \infty$ and find soliton and radiation parameters. Eqs. (25), (26) yield

$$T^{(\Gamma)} = \frac{1}{\Gamma} T_0 \quad \text{and} \quad P^{(\Gamma)} = \Gamma^2 P_0. \tag{27}$$

Note that with $\Gamma = e^{-\alpha Z}$ as above this reproduces perturbative result, Eq. (16). The soliton energy is then

$$E_{\rm sol}^{(\Gamma)} = \Gamma E_{\rm sol}, \tag{28}$$

and the radiation energy follows from

$$\lim_{n\to\infty} (\sqrt[2n]{\Gamma} - 1)^{2n} = 0 \tag{29}$$

so that

$$E_{\rm rad} = 0. \tag{30}$$

This result is quite remarkable: in the limit—and only in the limit—the soliton carries all the energy, and radiation has zero energy. This is so because when the number of splices n grows, the radiated energy at each splice scales as $1/n^2$ [see Eq. (11)]. Then the cumulative total radiative energy scales as $n \times 1/n^2$, which vanishes in the limit. This also confirms Ref. [24] where a quite different ansatz yields the same pulse amplitude and the absence of radiation if the power loss is slow.

A. An apparent contradiction

We have made no assumptions about the locations of the splices z_i, or the spatial distance Δz between them. We can therefore let these distances tend to zero, i.e., make the transition from distributed to localized loss. This implies that results from both cases must be equal. However, there is the contradiction that pulse parameters in Eqs. (27) and (22) are different, and so are soliton energies in Eqs. (21) and (28). It is highly instructive to get to the root cause of this apparent discrepancy.

To be sure, there are conservation laws for the lossless fiber segments between splices. In particular, constancy of the energies of both the soliton and the radiation, and thus also the sum of the two, is guaranteed. However, some other quantities are not preserved in these fiber segments. As the pulse shape breathes in the course of the beat between soliton and radiation, both peak power and pulse width oscillate, along with other quantifiers such as chirp factor, etc. We need to assess this breathing first, in order to gauge its impact. To do so, we look at both parts—solitonic and radiative—first, then combine the two. In the Appendix we will give an explicit

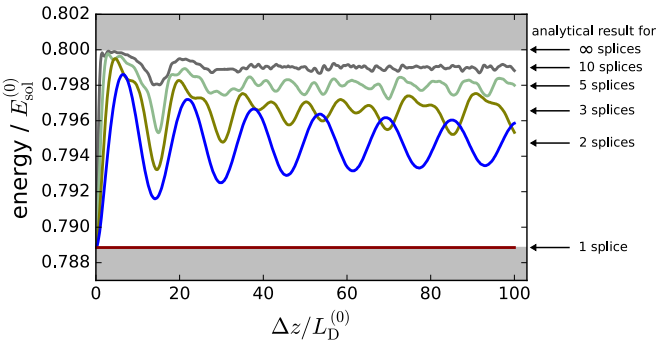

FIG. 1. Soliton energy after the first splice (bottom trace, or after the last of several splices (2, 3, 5, or 10 as indicated) when their separation Δz is varied. Here, $\Gamma = 0.8$. The strongest oscillation is found in the case of two splices. Arrows on the right mark the predicted asymptotic values according to Eq. (23) or, for distributed loss (infinite number of splices), from Eq. (28). Note that all curves start (for $\Delta z = 0$) at the level pertaining to a single splice, Eq. (21).

formulation of the evolving beat amplitude. The dispersive spreading of the radiative part gives rise to the decay of the beat note; the shifting phases give rise to the oscillation, which asymptotically has a spatial period of $4\pi L_{\rm D}$ [see Eq. (7)]. For an accurate description, the Gouy phase shift must also be taken into account.

When this evolving pattern arrives at the next splice, how will it be translated into a new soliton-plus-radiation combination? It takes many oscillation periods ($4\pi L_{\rm D}$) before the oscillation amplitude has fully died down. If the next splice occurs sooner than that, the position of the splice within the beat pattern does have an impact on the resulting pulse after that next splice. We find from numerical direct scattering transform that intercepting the beat at positions of high peak power translates to solitons with relatively lower energy, and vice versa. (In the case of gain, instead of loss, it is the other way around.) Therefore, the spatial distance between one splice and the next has a profound impact on the resulting soliton energy after the next splice.

In the case of more than two splices it may happen that the separation of splices might equal the distance over which the phase difference rotates through 2π. This would create resonances as described in Ref. [26], and would lead to a resonant enhancement of radiation. To avoid this resonance, we cannot make the splice distances shorter: then not the next splice but some subsequent splice would get into resonance. We can only make the distance larger. Figure 1 shows the evolution in the case of one or several splices. These data were obtained as follows: from numerical simulation we find the pulse shape after the splice and subject it to direct scattering transform to find the energy of the resulting soliton. The slow decay of the oscillation in the case of two splices is clearly visible; the picture confirms that it has not died down unless $\Delta z \gg 4\pi L_{\rm D}$.

If there are more than two splices, even if they are physically equidistant, they are not equidistant with respect to the relevant length scales as the latter also change with remaining energy. It is therefore not surprising that for three or more splices the oscillation dies down sooner. The situation is akin to a reflection off a chirped grating: there is no sharp resonance. Still, some finite minimum decay distance Δz always remains; therefore, in the limit that the number of splices diverges, the total length—as the sum of infinitely many finite distances—also diverges.

This shows that our result Eq. (27), which coincides with the perturbative result, necessarily requires $L_\alpha \to \infty$, i.e., vanishing loss per finite length. The advantage of our treatment is that we now see beyond that limit, and understand why this condition is necessary: there must be sufficient propagation distance for interferences to die down. We can also specify quantitatively what happens if the loss is stronger.

All curves in Fig. 1 approach the markers (arrow on the right) labeled with the appropriate number of splices, which corroborates Eq. (23). As the number of splices tends to infinity, the curves tend to Γ. Also, at $\Delta z = 0$ (all splices collapsed into one position) they all begin at the marker for the single splice, $2\sqrt{\Gamma} - 1$. This resolves the apparent contradiction that stepwise and distributed loss are not the same, but should coincide when Δz is zero.

The fact that we recovered the perturbational results for pulse peak and width is therefore coupled to the requirement that $L_\alpha \to \infty$, which is the same assumption that must be made for perturbational analysis. The recovery is therefore no surprise. However, with our current approach we have both a physical reason (the beat must decay before the next splice so that radiative contributions can simply be added up) and the means to go beyond the limiting case, into more realistic situations.

B. An interesting observation

Finite loss represents a deviation from strict adiabaticity, or some degree of diabaticity. We suggest to introduce the degree of diabaticity $\mathcal{D}$ as the ratio of the applicable dispersion length and the loss length. The applicable dispersion length is the one that refers to the soliton alone; it can vary during propagation as the total energy decays and the pulse duration adapts to that. Thus,

$$\mathcal{D}(z) = \frac{L_{\rm D}(z)}{L_\alpha}. \tag{31}$$

With small nonzero diabaticity ($\mathcal{D} \ll 1$) the soliton is constantly askew and never quite reaches a new equilibrium between dispersive and nonlinear effects, normally the hallmark of solitons. It is in this situation that this near soliton displays some chirp, and radiation is produced continuously.

Figure 2 shows the generated radiation accumulated over distance z. For this figure we numerically propagated a pulse, which initially was an $N = 1$ soliton in the presence of diabaticity as indicated. Right after starting at $z = 0$, the curves rise and, as radiation quickly exceeds its initial level, grow fastest for the strongest diabaticity. Wiggles in the curves reflect the beating as described above. Disregarding these and also the initial transient, the radiation seems to increase roughly exponentially with distance as the nearly straight curves in this semilog plot indicate. This is again a consequence of the dynamic evolution not only of the energy, but also of $L_{\rm D}$. With

$$\frac{L_{\rm D}(z)}{L_\alpha} = \frac{L_{\rm D}(0)}{L_\alpha}\, e^{2z/L_\alpha} \tag{32}$$

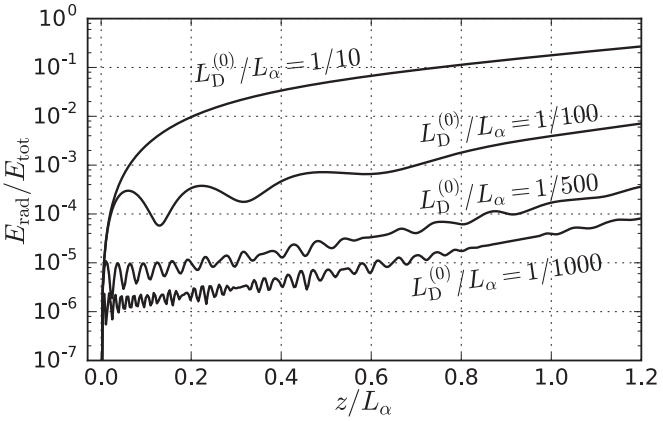

FIG. 2. Relative amount of radiation during propagation for different ratios of $L_D^{(0)}/L_\alpha$. Propagation distance is scaled to L_α.

the ratio $\mathcal{D} = L_D/L_\alpha$ in Fig. 2 grows from launch point to fiber end by a factor $\exp(2.4) \approx 11$.

Close inspection of the traces in Fig. 2 reveals that an extrapolation of the traces back to $z = 0$ yields radiative energy values, which, within accuracy limits, coincide with the square of the respective curve's parameter. For example, the $L_D^{(0)}/L_\alpha = 1/100$ curve seems to emerge from $E_{rad}/E_{tot} = 10^{-4}$, etc. When we checked this at positions other than $z = 0$, we made a remarkable empirical observation. In the moderately diabatic case as shown in Fig. 2, disregarding the transient and the wiggles, the fraction of accumulated radiative energy at position z is quite closely given by

$$\frac{E_{rad}^{(z)}}{E_{tot}^{(z)}} = (\mathcal{D}(z))^2 = \left(\frac{L_D(z)}{L_\alpha}\right)^2. \tag{33}$$

We tested this observation with numerical simulations. Starting from initial values of $\mathcal{D}$ in the range $10^{-4} \leqslant \mathcal{D}(0) \leqslant 10^{-2}$, we used a split-step Fourier code to numerically propagate solitons of order N over a distance of $3L_\alpha$. Then we performed direct scattering analysis for 32 intermediate points of each propagation. The results are shown in Fig. 3.

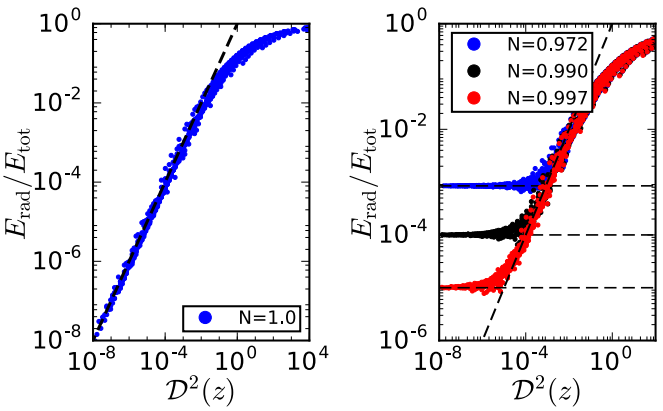

FIG. 3. Fraction of energy going into radiation. Data points obtained from propagation simulations over a distance of $3L_\alpha$ using initial values of $\mathcal{D}$: $10^{-4} \leqslant \mathcal{D}(0) \leqslant 10^{-2}$. Launch condition: $N = 1$ soliton (left), $N < 1$ (right).

In the left panel of Fig. 3, an $N = 1$ soliton was launched into a lossy fiber. In the other panel, pulses were launched with $N \neq 1$ as indicated. In each case, the diagonal lines are plots of Eq. (33), and horizontal lines indicate the initial radiation according to Eq. (11).

For all $N \neq 1$ shown, the initial radiation dominates at small $\mathcal{D}$, while radiation generated during diabatic propagation dominates for large $\mathcal{D}$. The break point indicates where the continuously rising part begins to swamp the constant initial value. The continuously generated radiation follows Eq. (33) quite closely as long as one considers the near-adiabatic regime. Once radiation becomes a sizable fraction of the total energy, saturation sets in because the radiative fraction of the total energy obviously cannot go beyond 100% [as Eq. (33) seems to suggest]. The onset of saturation marks the limit of applicability of Eq. (33).

C. Rate of generation of radiation

We calculate the local rate of generation of radiation from the cumulative value of Eq. (33). The growth rate from position z to $z + dz$ is found from

$$\frac{dE_{rad}^{(z)}}{E_{tot}^{(z)}} = \left(\frac{L_D^{(z+dz)}}{L_\alpha}\right)^2 - \left(\frac{L_D^{(z)}}{L_\alpha}\right)^2. \tag{34}$$

Using the change of pulse duration over infinitesimal distance $T^{(z+dz)} \approx e^{\alpha\, dz}\, T^{(z)}$ in the adiabatic approximation, this leads to

$$\frac{dE_{rad}^{(z)}}{dz} = E_{tot}^{(z)}\, [\mathcal{D}(z)]^2\, \frac{4}{L_\alpha}. \tag{35}$$

This growth rate is proportional to the square of diabaticity, and it is referred to L_α as its natural length scale; both are reasonable. This has been derived for the near-adiabatic regime, and that is why it predicts proportionality to the total rather than the physically more plausible soliton energy. For the same reason Eq. (35) does not reflect the saturation seen in Fig. 3.

D. Demise of a soliton

We have argued that the degree of diabaticity increases even when the loss factor in terms of loss per km is constant because the relevant length scale L_D keeps growing as power keeps bleeding away from the soliton. As $L_D(z)$ becomes larger, the loss per L_D naturally increases until the loss per L_D is no longer small. Eventually, all propagation in lossy fiber must run into the regime of strong diabaticity; it was argued in Ref. [22] that this leads to the decay of the soliton.

Figure 4 shows the decay of E_{sol} for various $\mathcal{D}(0)$ values. All traces have the same general structure: For some length they remain quite close to the dashed straight line, which describes Beer's law and the adiabatic case, but eventually they begin to depart from it; a little further on they plummet to zero. It makes sense to divide the decay process into two stages, the near-adiabatic phase over distance z_a, and the diabatic phase over distance z_d. The crossover point between the two remains ill defined from inspection of Fig. 4 alone, but surely it must be characterized by some specific value of the local degree of diabaticity $\mathcal{D}(z_a)$, which remains to be determined below.

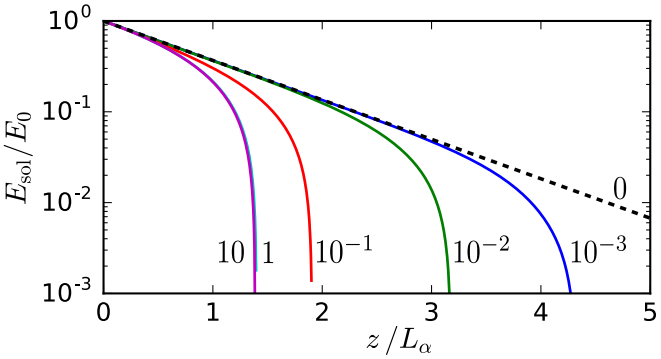

FIG. 4. Decay of soliton energy in a lossy fiber, with $\mathcal{D}(0)$ as a parameter. Curves for $\mathcal{D}(0) \geqslant 1$ practically coincide. Dashed line is for the adiabatic case. Decay is near adiabatic at first, but later becomes loss dominated.

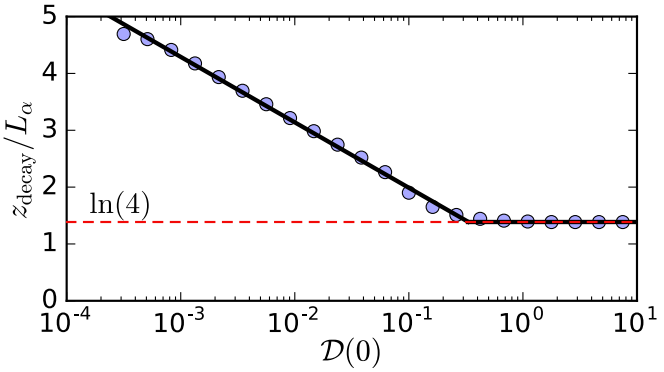

FIG. 5. Decay distance of solitons when $\mathcal{D}(0)$ is varied. Two regimes are clearly visible: prediction by Eq. (40) for small $\mathcal{D}(0)$ and by Eq. (41) for large $\mathcal{D}(0)$. The crossover point is located at $\mathcal{D}(z_{\rm a}) = 0.33$.

Writing $\mathcal{D}(z_{\rm a})$ in terms of $\mathcal{D}(0)$ and L_α, one finds

$$z_{\rm a} = -\frac{L_\alpha}{2}\,\ln\!\left(\frac{\mathcal{D}(0)}{\mathcal{D}(z_{\rm a})}\right). \tag{36}$$

When entering the diabatic phase at $z = z_{\rm a}$ the soliton loses its ability to adapt to the energy loss.

Considering Eq. (9) we can write its shape as

$$A(z,t) = N\sqrt{P_0}\,\mathrm{sech}\!\left(\frac{t}{T_0}\right)\,\exp\!\left(-\frac{\alpha}{2}\,z\right). \tag{37}$$

With rapid decay the soliton is unable to reshape so that T_0 is constant; then, Eq. (3) shows that $\sqrt{P_0}$ is also constant. The loss term on the far right-hand side multiplies the soliton order N to form an effective soliton order N':

$$N' = N\exp\!\left(-\frac{\alpha}{2}\,z\right). \tag{38}$$

The soliton disappears as soon as this dips below $N' = 1/2$. Inserting this value in Eq. (38) we have

$$z_{\rm d} = L_\alpha\,\ln(4) \quad \text{if } N = 1. \tag{39}$$

The entire distance from launch to demise is then $z_{\rm a} + z_{\rm d}$, i.e.,

$$z_{\rm decay} = L_\alpha\left[\ln(4) - \frac{1}{2}\,\ln\!\left(\frac{\mathcal{D}(0)}{\mathcal{D}(z_{\rm a})}\right)\right] \tag{40}$$

if $z_{\rm a} \geqslant 0$. If formally $z_{\rm a} < 0$ there is no adiabatic phase, and the decay length is $z_{\rm d}$ alone:

$$z_{\rm decay} = z_{\rm d} = L_\alpha\ln(4) \quad \text{if} \quad z_{\rm a} < 0. \tag{41}$$

The result of this analysis is shown together with numerical data in Fig. 5.

The horizontal line at ln(4) represents the diabatic case of Eq. (41). Data points in that regime are very close to the prediction. The slanted line represents the adiabatic case of Eq. (40). The slope agrees very well with data points. We shifted the curve by variation of the unknown $\mathcal{D}(z_{\rm a})$ to fit the data points. We find the best value as the location of the intersection at $\mathcal{D}(z_{\rm a}) = 0.33$. Note that this value describes the transition point to saturation in Fig. 3 quite well.

The interpretation of all this is that the soliton reaches a point of no return at $z = z_{\rm a}$; thereafter its decay proceeds so rapidly that it has no chance to adjust. At $z = z_{\rm decay}$ its energy has fully been radiated off.

This analysis requires a slight modification when an $N \neq 1$ soliton is launched. By reinserting the definition of $\mathcal{D}(0)$ in Eq. (40) we see that it contains a factor T_0^2. We are dealing here with rapid decay in the strongly adiabatic case so that we can use Eq. (22) to replace T_0 with $T_0/(2N-1)^2$. With that, Eq. (40) is modified into

$$z_{\rm decay} = L_\alpha\left[\ln(4) - \frac{1}{2}\,\ln\!\left(\frac{\mathcal{D}(0)}{\mathcal{D}(z_{\rm a})(2N-1)^2}\right)\right]. \tag{42}$$

For the strongly diabatic case, we reconsider Eq. (38) for $N \neq 1$ and obtain that Eq. (41) is replaced with

$$z_{\rm decay} = L_\alpha\,\ln(4N^2). \tag{43}$$

This can be checked against the result in Ref. [22] where an $N = 1.4$ soliton was considered with an initial diabaticity value of $\mathcal{D}(0) = 7.4\times10^{-4}$. The soliton was numerically found to decay at $z_{\rm decay} \approx 110\text{km} = 5.07\,L_\alpha$. Our Eq. (42) yields $z_{\rm decay} = 109.2\text{km} = 5.03L_\alpha$, which is in perfect agreement.

IV. CONCLUSION

Solitons are defined by a dynamical equilibrium between linear (dispersive) and nonlinear influences. As soon as the diabaticity differs from zero, i.e., as soon as there is more than infinitesimal loss, this equilibrium is never quite reached, and the pulse remains off balance. Then, a continuous bleeding of energy ultimately leads to the disappearance of the soliton. We discussed how a soliton readjusts its properties in the presence of slow perturbations acting on it. By carefully assessing the interplay between soliton and radiation, we have described the reshaping of the pulse with analytic and numeric tools. If the diabaticity gets too large, the soliton is so much distorted that its very concept begins to become ill defined. Our results are checked against numerical simulation and hold very well.

Luckily the concept of solitons does not immediately become useless when the underlying equation becomes non-integrable. Physically, the concept of a pulse that balances nonlinearity and dispersion makes sense even in the presence of parameter variation, such as energy loss. Our discussion

allows us to find the soliton's parameters for loss weak or strong, localized or distributed. Its eventual decay in a lossy fiber is quantitatively determined. We point out that our treatment can be generalized. If the modification occurs not in pulse peak power but in, say, γ, β_2, or T_0 [the other quantities in Eq. (4)], the same logic as presented here is applicable, because any such change can be written as a modification of N. Therefore our ansatz can address the fate of a soliton at a joint between unlike fibers, etc.

Finally, we remark that solitons are self-stabilizing entities distinct from their environment. They may thus serve as the absolute minimum requirement models for living organisms, which are entities that perpetually exchange energy and matter with their environment, and yet are clearly distinct from it. While organisms may be able to adapt to slow environmental changes, they may not be able to cope with rapid change. Our treatment demonstrates the difference between sudden and gradual changes in a fully tractable situation, and it highlights the key role of the rate of change. As global warming progresses, there may be important lessons for us to be learned.

ACKNOWLEDGMENT

We enjoyed fruitful discussions with Uwe Bandelow and Boris Malomed.

APPENDIX: SOLITON-RADIATION BEAT AMPLITUDE

If parameters of a pulse deviate slightly from that of a soliton, it will evolve with oscillating peak power. This fact was first reported by Satsuma and Yajima [2] from numerical calculations; they also showed that the oscillation amplitude decays as $1/\sqrt{z}$. The oscillation is a beat between soliton and radiation; it evolves according to the difference in phase evolutions of soliton and radiation. After sufficient distance the radiation is dispersed away, and the oscillation subsides. Then the soliton itself becomes visible [13,17,21].

Several authors have sought a description of the decaying oscillation amplitude. In Ref. [18] a Lagrangian approach was used to derive very approximate equations, and in Ref. [14] expressions were found by perturbation analysis. We give a physically motivated description, which provides more insight than previously obtained, and is more accurate.

The scaling of the beat amplitude decay can be understood as follows: the solitonic part has constant amplitude $\sqrt{P_1}$. The radiative part spreads out; in the far field ($z \gg L_D$) it widens linearly with distance. As its power is also preserved, its amplitude at pulse center droops like $1/\sqrt{z}$; that determines the beat amplitude. This reproduces the scaling reported in Ref. [2].

The evolution of the beat note begins at the moment when the initial soliton with peak power P_0 exits the splice. At this point we have a pulse of the same shape (sech) and chirp (none) as the pure soliton before the attenuation because the attenuation does not change these parameters. Initially right after the splice the pulse now has a peak power of $N^2 P_0$. However, we know that it consists of a soliton with peak power P_1 and a nonzero contribution of radiation. In the case of loss, in this first moment the pulse's peak power has its global maximum, which tells us that initially both parts, solitonic and radiative, are in phase with each other at least in the center. In the case of gain, it is the other way around: a global minimum indicates opposite phase.

The radiative part is subject to dispersive broadening. To describe its phase and amplitude evolution, we can conveniently exploit the similarity of the dispersion with diffraction, keeping in mind that dispersion is diffraction's one-dimensional counterpart. In the analogy, the pulse starts from a position analogous to a beam waist (plane wavefronts correspond to zero chirp). In the absence of a closed expression for the dispersive evolution of a sech pulse, we greatly simplify the task by one approximation: we assume the shape of the dispersive part to be Gaussian. Then it has a dispersive evolution of the form

$$U(z,t)_{\mathrm{disp}} = \frac{AT_0}{\sqrt{T_0^2 - i\beta_2 z}} \exp\left[-\frac{t^2}{2\left(T_0^2 - i\beta_2 z\right)}\right], \quad \text{(A1)}$$

where the scaling factor A is given by the amplitude difference between the initial pulse and the resulting soliton,

$$A = (1 - N)\sqrt{P_0}. \quad \text{(A2)}$$

From Eq. (A1) we obtain the amplitude and phase at the temporal center $t = 0$

$$|U_{\mathrm{disp}}(z,0)| = \frac{T_0}{\sqrt[4]{T_0^4 + \kappa\beta_2^2 z^2}}, \quad \text{(A3)}$$

$$\varphi_{\mathrm{disp}}(z,0) = -\tfrac{1}{2}\arctan(\kappa\gamma P_0 z), \quad \text{(A4)}$$

where we need to introduce a stretch factor κ to achieve similarity of the Gaussian to the original sech shape, because a sech(t/T_0) has a quite different pulse width than a Gaussian with width T_0. The evolution of $\varphi_{\mathrm{disp}}(z,0)$ describes the Gouy phase [27], which in a single dimension amounts to one half of its value in the more familiar case of two dimensions [28].

The dispersive part beats with the underlying soliton. The beat note is determined by the phase difference between the linearly evolving soliton and the dispersive part,

$$\begin{aligned}\Delta\varphi(z,0) &= \varphi_{\mathrm{sol}}(z,0) - \varphi_{\mathrm{disp}}(z,0) \\ &= \frac{\gamma P_1}{2} z + \frac{1}{2}\arctan(\kappa\gamma P_0 z). \end{aligned} \quad \text{(A5)}$$

With the scaling factor from Eq. (A2), the dispersive amplitude Eq. (A3), and the phase difference Eq. (A5) we can write

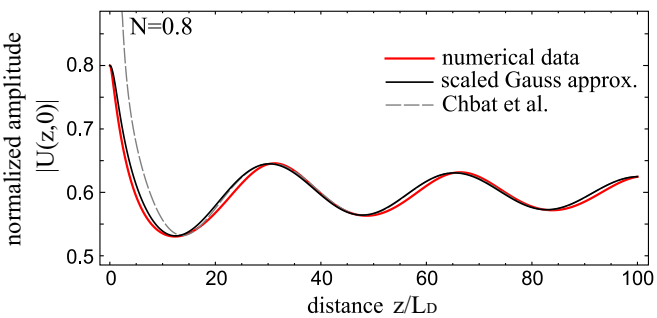

FIG. 6. Evolution of the beat pattern after the first splice. Red line: numerical simulation; solid black line: Gaussian approximation with empirical correction factor; dashed line: solution from Ref. [14].

the beat amplitude evolution as that of the soliton with an oscillating dispersive part on top of it:

$$|U(z,0)| = \sqrt{P_1} + \sqrt{P_0}(1-N)\,\frac{T_0}{\sqrt[4]{T_0^4 + \kappa\beta_2^2 z^2}} \times \cos\left(\frac{\gamma P_1}{2} z + \frac{1}{2}\arctan\left(\kappa\gamma P_0 z\right)\right). \quad \text{(A6)}$$

As the solitonic part has constant amplitude $\sqrt{P_1}$, the beat amplitude is determined by the evolution of the radiation amplitude. As radiation disperses, it gets diluted, and its amplitude at the overlap decays. The beat note amplitude is proportional to the amplitude of the radiation itself, which evolves in the far field as $1/\sqrt{z}$, which, again, reproduces the scaling in Ref. [2].

Figure 6 shows the beat note amplitude for $N = 0.8$. In lieu of an exact solution, a numerical simulation (red line) serves as the reference. Our result in the Gaussian approximation with $\kappa = 0.42$ is shown as a black line. Both curves start at amplitude N and asymptotically tend to $2N - 1$ as required. The agreement is very close indeed. Also shown is the perturbative result from Ref. [14] (dashed line); while it fails in the early phase, it is also quite good later on.

[1] V. E. Zakharov and A. B. Shabat, Zh. Eksp. Teor. Fiz. **61**, 118 (1971) [Sov. Phys. JETP **34**, 62 (1972)].
[2] J. Satsuma and N. Yajima, Suppl. Progr. Theor. Phys. **55**, 284 (1974).
[3] A. Hasegawa and F. Tappert, Appl. Phys. Lett. **23**, 142 (1973).
[4] L. F. Mollenauer, R. H. Stolen, and J. P. Gordon, Phys. Rev. Lett. **45**, 1095 (1980).
[5] W. Forysiak, *16th Annual Meeting of the IEEE, LEOS Lasers and Electro-Optics Society* (IEEE, Piscataway, 2003), p. ThI2.
[6] V. I. Karpman and E. M. Maslov, Zh. Eksp. Teor. Fiz. **73**, 537 (1977) [Sov. Phys. JETP **46**, 281 (1977)].
[7] Y. Kodama and A. Hasegawa, Opt. Lett. **7**, 339 (1982).
[8] K. J. Blow and N. J. Doran, Opt. Commun. **42**, 403 (1982).
[9] K. J. Blow and N. J. Doran, Opt. Commun. **52**, 367 (1985).
[10] A. Hasegawa and Y. Kodama, Proc. IEEE **69**, 1145 (1981).
[11] D. J. Kaup, SIAM J. Appl. Math. **31**, 121 (1976).
[12] H. Kubota and M. Nakazawa, IEEE J. Quant. Electron. **26**, 692 (1990).
[13] M. Böhm and F. Mitschke, Phys. Rev. E **73**, 066615 (2006).
[14] M. W. Chbat, P. R. Prucnal, M. N. Islam, C. E. Soccolich, and J. P. Gordon, J. Opt. Soc. Am. B **10**, 1386 (1993).
[15] G. P. Agrawal, *Nonlinear Fiber Optics*, 5th ed. (Academic Press, New York, 2013)
[16] F. Mitschke, *Fiber Optics. Physics and Technology*, 2nd ed. (Springer, Berlin, 2016).
[17] J. P. Gordon, J. Opt. Soc. Am. B **9**, 91 (1992).
[18] W. L. Kath and N. F. Smyth, Phys. Rev. E **51**, 1484 (1995).
[19] G. Boffetta and A. Osborne, J. Comput. Phys. **102**, 252 (1992).
[20] M. I. Yousefi and F. R. Kschischang, IEEE Trans. Inf. Theory **60**, 4329 (2014).
[21] M. Böhm and F. Mitschke, Appl. Phys. B **86**, 407 (2007).
[22] M. Böhm and F. Mitschke, Phys. Rev. A **76**, 063822 (2007).
[23] W.-J. Liu, X.-C. Lin, and M. Lei, J. Mod. Opt. **60**, 932 (2013).
[24] R. K. Bullough, A. P. Fordy, and S. V. Manakov, Phys. Lett. A **91**, 98 (1982).
[25] K. J. Blow and N. J. Doran, in: *Optical Solitons - Theory and Experiment*, edited by J. R. Taylor (Cambridge University Press, Cambridge, 1992).
[26] L. F. Mollenauer, J. P. Gordon, and M. N. Islam, IEEE J. Quant. Electron. **22**, 157 (1986).
[27] A. E. Siegman, *Lasers* (University Science Books, Herndon, 1986).
[28] S. Feng and H. G. Winful, Opt. Lett. **26**, 485 (2001).